BOUNDARY SUMMATION EQUATIONS

Per Sundqvist

30th September 2004

Department of Scientific Computing, Information Technology, Uppsala University, Box 337, SE-751 05 Uppsala, Sweden. email: per.sundqvist@it.uu.se

Abstract.

A new solution method for systems of partial difference equations is presented. It can be seen as a discrete counterpart of boundary integral equations, but with sums instead of integrals. The number of unknowns in systems of linear difference equations with constant coefficients defined on uniform d-dimensional grids are reduced so that one dimension is eliminated.

The reduction is obtained using fundamental solutions of difference operators, yielding a reduced system that is dense. The storage of the reduced system requires $\mathcal{O}(N)$ memory positions, where N is the length of the original vector of unknowns. The application of the matrix utilizes fast Fourier transform as its most complex operation, and requires hence $\mathcal{O}(N \log N)$ arithmetic operations.

Numerical experiments are performed, exploring the behavior of GMRES when applied to reduced systems originating from discretizations of partial differential equations. Model problems are chosen to include scalar equations as well as systems, with various boundary conditions, and on differently shaped domains. The new solution method performs well for an upwind discretization of an inviscid flow-problem.

A proof of grid independent convergence is given for a simpler iterative method applied to a specific discretization of a first order differential equation. The numerical experiments indicate that this property carries over to many other problems in the same class.

Key words: Fundamental solutions, partial differential equations, partial difference equations, boundary methods.

1 Introduction

The purpose of this paper is to describe a new solution method for partial difference equations. The target problem is one that can be represented by a sparse coefficient matrix where most rows are equal, up to translations. Using fundamental solutions of difference operators, we reduce the original, sparse system into a much smaller but dense linear system. Our main contributions are the reduction process in itself and an efficient technique for applying the reduced system matrix. The numerical experiments in the paper utilizes these by solving reduced systems iteratively by GMRES.

Two very desirable properties are obtained by the reduction. The first is the decreased number of unknowns, which e.g. reduces the maximal dimensionality of the Krylov subspace determined by GMRES. The other property is that GMRES requires less iterations when applied to the reduced system, than to the original one. Taken together, these properties enable us to use full GMRES in the numerical experiments.

In order to introduce our method and to put it in perspective, we take a detour around partial differential equations (PDEs). Approximate solutions of PDEs are commonly determined using finite difference, finite element, or finite volume methods. If the PDE is linear with constant coefficients, it can be reformulated into an integral equation, where the unknown is a function on the boundary of the domain of interest. Such boundary integral equations (BIE) are used in the boundary element method (BEM), where the BIE is discretized. The resulting system is dense, but can often be solved iteratively by the use of fast matrix-vector multiplication techniques, see e.g. [6], [8] or [14]. The use of algebraic multi-grid preconditioners has been proposed, see [11].

The derivation of a BIE relies on specific properties of the differential operator, such that a fundamental solution is explicitly known. Existence of well behaved fundamental solutions is proved for linear differential operators with constant coefficients in [9], but the construction is often very difficult.

Another solution method for PDEs is the method of fundamental solutions (MFS). For a survey with many references, see [4]. It is mainly used for elliptic problems, and the idea is to determine a linear combination of translated fundamental solutions, such that given boundary conditions are satisfied, either exactly, or in a least squares sense. As the name suggests, the MFS depends on that a fundamental solution is known.

Both the BEM and the MFS can be referred to as boundary methods for PDE problems. The concept of fundamental solutions is defined also for linear *difference* operators with constant coefficients, and existence is proved in [3]. To distinguish fundamental solutions of differential and difference operators, we will sometimes call the latter discrete fundamental solutions. Until very recently, only a few discrete fundamental solutions have been known, implying that existing boundary methods for difference equations either have been derived by alternative procedures, such as in the method of difference potentials, see [13], or in a very problem specific setting, such as the boundary algebraic equations for lattice problems in [12].

In [2], discrete fundamental solutions are constructed using fast Fourier transform (FFT), yielding an $\mathcal{O}(N \log N)$ algorithm that works even when the symbol of the difference operator has zeros.

The approach in this paper is to use discrete fundamental solutions to derive a boundary method for difference equations. This new method is not problem specific, thanks to the generality of the algorithm in [2]. As for BEM, the resulting system is dense, but there are several differences. One is that our method is defined not only for discretized PDE problems, but for any sparse linear system that can be represented by a constant difference operator with

boundary conditions. One non-PDE example is the class of banded multi-level Toeplitz matrices. Another difference is that, if the original problem is a PDE, we first discretize the problem and then reduce the discretization to the boundary. The BEM approach is to discretize the integral equations that are obtained when reducing the PDE to a BIE.

A similarity with the MFS approach is that what we really determine are the coefficients in a linear combination of translated fundamental solutions, although we use discrete ones. A difference is that the treatment of inhomogeneous equations is straight forward using our method, whereas a non-zero right hand side must be eliminated by the computation of a particular solution when using MFS.

The method we present requires a uniform grid. If the difference equation is a discretization of a PDE posed on a non-rectangular domain, we suggest an embedded boundary technique. This way, we obtain a fast technique for applying the reduced matrix, making many iterative solution methods available.

The paper is organized as follows. Sections 2 to 4 describe the problems we treat, how the reduction process is performed and how the reduced system can be solved. Section 5 relates the reduced system to BIE. Experiments on scalar PDE-problems on the unit square are performed in section 6, and in section 7 we prove grid independent convergence for a model problem. The remaining sections contain numerical experiments exploring generalizations in different directions; non-square regions in section 8, higher dimensions in section 9, and systems of PDE in section 10.

2 Problem Formulation

The problems we consider arise e.g. when a linear PDE with constant coefficients is discretized using finite differences on a uniform grid. The discretization consists of a difference operator which we denote by $\hat{P}$, and boundary conditions. Such a problem can be represented by a linear system of equations,

$$Pu = f. \tag{2.1}$$

The unknowns u_i are indexed using a d-dimensional index $i = (i_1, \ldots, i_d)$, such that $i \in \bar{\Omega} \subset \mathbb{Z}^d$, for which it holds

$$\bar{\Omega} = \Omega \cup \Gamma, \quad \Omega \cap \Gamma = \emptyset,$$

where Ω contains the interior grid-points where the difference operator can be applied without modification. The remaining grid-points belong to Γ, and are those where boundary conditions are imposed or $\hat{P}$ needs to be modified due to its extension.

The unknown grid-function u is allowed to be vector valued, with n_c components in each grid-point. The stencil of $\hat{P}$ has weights that are $n_c \times n_c$ matrices, and we can express the difference operator as

$$\hat{P}v_i = \sum_{j \in S} B_j v_{i-j}, \quad i \in \Omega, \tag{2.2}$$

where B_j are the weight matrices and S is the set of indices j for which B_j is non-zero. For example, if $\hat{P}$ is the discrete Laplacian in two dimensions, $S = \{(0,0),(0,\pm1),(\pm1,0)\}$ and $B_{(0,0)} = -4$, $B_{(0,\pm1)} = B_{(\pm1,0)} = 1$.

In general, the coefficient matrix P is $N \times N$, where $N = n_c N_{\bar{\Omega}}$ and $N_{\bar{\Omega}}$ is the number of elements in $\bar{\Omega}$. Correspondingly, N_Γ and N_Ω denote the number of elements in Γ and Ω.

Ordering the unknowns in u such that all grid points in Γ come first, yields the following partitioning of (2.1):

$$\begin{pmatrix} P_\Gamma & P_{\Gamma\Omega} \\ P_{\Omega\Gamma} & P_\Omega \end{pmatrix} \begin{pmatrix} u_\Gamma \\ u_\Omega \end{pmatrix} = \begin{pmatrix} f_\Gamma \\ f_\Omega \end{pmatrix}. \tag{2.3}$$

The block row $\begin{pmatrix} P_\Gamma & P_{\Gamma\Omega} \end{pmatrix}$ represents the equations that can be referred to as boundary conditions and $\begin{pmatrix} P_{\Omega\Gamma} & P_\Omega \end{pmatrix}$ represents $\hat{P}$.

As remarked in the introduction, our method is not restricted to equations originating from PDE problems. If (2.1) is a banded multi-level Toeplitz system, it can be reordered to fit (2.3) by letting $\begin{pmatrix} P_\Gamma & P_{\Gamma\Omega} \end{pmatrix}$ contain the rows which are disturbed due to that the matrix is a finite section of an infinite Toeplitz matrix.

3 Derivation of the Reduced System

Our goal is to reduce (2.3) to a linear system of the same size as P_Γ, and to do this we use a fundamental solution of the difference operator $\hat{P}$. Such a discrete fundamental solution is denoted by E and is a matrix valued grid function that satisfies

$$\hat{P}E_i = \delta_i I \equiv \begin{cases} I & i = 0 \\ 0 & i \neq 0 \end{cases}, \tag{3.1}$$

where I is the identity matrix of size n_c. The fundamental solution is used in a convolution operator $\hat{K}$, defined by

$$\hat{K}u_i = \sum_{j \in \bar{\Omega}} E_{i-j} u_j, \qquad i \in \bar{\Omega}, \tag{3.2}$$

where E_{i-j} denotes E in grid-point $x_i - x_j$.

To compute the values of E needed in (3.2), we solve (3.1) on a domain that is about 2^d times larger than $\bar{\Omega}$. Two strategies for the construction of E is described in [2] and are briefly reviewed here. Since E is used only on a bounded domain, we are free to choose boundary conditions outside that domain. Both strategies impose periodic boundary conditions in $d-1$ dimensions and use the discrete Fourier transform do decouple the system into a number of smaller sparse systems. Different fundamental solutions are obtained, depending on what additional conditions are imposed on the smaller systems. The first strategy is to impose Dirichlet boundary conditions, and the resulting fundamental solution will here be denoted E^D. The second strategy uses no particular boundary conditions, but solves the smaller systems, which are under-determined, in

a least squares sense, yielding a fundamental solution which we denote E^L. In cases where it does not matter which fundamental solution we use, we simply write E.

To derive the reduced system, we need the following theorem

THEOREM 3.1. *Let* $\begin{pmatrix} P_{\Omega\Gamma} & P_\Omega \end{pmatrix}$ *be defined as in (2.3). Then*

$$\begin{pmatrix} P_{\Omega\Gamma} & P_\Omega \end{pmatrix} \begin{pmatrix} K_\Gamma & K_{\Gamma\Omega} \\ K_{\Omega\Gamma} & K_\Omega \end{pmatrix} = \begin{pmatrix} 0 & I \end{pmatrix},$$

where $\begin{pmatrix} K_\Gamma & K_{\Gamma\Omega} \\ K_{\Omega\Gamma} & K_\Omega \end{pmatrix}$ *represents (3.2) with the same enumeration and partitioning as in (2.3).*

PROOF. The matrix product applied to an arbitrary vector can be expressed using operator notation, and we see that

$$\begin{aligned} \hat{P}\hat{K}v_i &= \sum_{j\in S} B_j \sum_{k\in\bar{\Omega}} E_{i-j-k} v_{i-j} = \sum_{k\in\bar{\Omega}} \sum_{j\in S} B_j E_{i-j-k} v_{i-j} \\ &= \sum_{k\in\bar{\Omega}} \delta_{i-k} I v_k, \quad i \in \Omega. \end{aligned} \tag{3.3}$$

□

Hence, by substituting

$$\begin{pmatrix} u_\Gamma \\ u_\Omega \end{pmatrix} = \begin{pmatrix} K_\Gamma & K_{\Gamma\Omega} \\ K_{\Omega\Gamma} & K_\Omega \end{pmatrix} \begin{pmatrix} v_\Gamma \\ v_\Omega \end{pmatrix} \tag{3.4}$$

in (2.3), we obtain

$$\begin{pmatrix} P_\Gamma K_\Gamma + P_{\Gamma\Omega} K_{\Omega\Gamma} & P_\Gamma K_{\Gamma\Omega} + P_{\Gamma\Omega} K_\Omega \\ 0 & I \end{pmatrix} \begin{pmatrix} v_\Gamma \\ v_\Omega \end{pmatrix} = \begin{pmatrix} f_\Gamma \\ f_\Omega \end{pmatrix}.$$

We immediately see that $v_\Omega = f_\Omega$, and the remaining equation for v_Γ is the reduced system

$$A v_\Gamma = g, \tag{3.5}$$

where

$$\begin{aligned} A &= P_\Gamma K_\Gamma + P_{\Gamma\Omega} K_{\Omega\Gamma} \qquad \text{and} \\ g &= f_\Gamma - (P_\Gamma K_{\Gamma\Omega} + P_{\Gamma\Omega} K_\Omega) f_\Omega. \end{aligned} \tag{3.6}$$

For clarity, we end the section by stating which operators correspond to the different K-blocks:

$$\begin{aligned} K_\Gamma v_\Gamma &\leftrightarrow \textstyle\sum_{j\in\Gamma} E_{i-j} v_j, \quad i \in \Gamma, \\ K_{\Omega\Gamma} v_\Gamma &\leftrightarrow \textstyle\sum_{j\in\Gamma} E_{i-j} v_j, \quad i \in \Omega, \\ K_{\Gamma\Omega} v_\Omega &\leftrightarrow \textstyle\sum_{j\in\Omega} E_{i-j} v_j, \quad i \in \Gamma, \\ K_\Omega v_\Omega &\leftrightarrow \textstyle\sum_{j\in\Omega} E_{i-j} v_j, \quad i \in \Omega. \end{aligned} \tag{3.7}$$

4 Computational Aspects

The reduced system is considerably smaller than the original one, but it is dense. Assume that (2.1) is posed on a d-dimensional hypercube with $n+1$ grid points in each dimension, implying $N = n_c(n+1)^d$. Assume also that the set of boundary grid points Γ consists of the hypersurfaces bounding the hypercube. The size of the reduced system (3.5) will then be

$$n_c N_\Gamma = n_c((n+1)^d - (n-1)^d) = \mathcal{O}(n_c d n^{d-1}),$$

and an explicit construction of A would require $\mathcal{O}(n_c^2 N_\Gamma^2)$ arithmetic operations and memory positions. In most situations, this is not acceptable, at least not if $d > 2$. However, the action of A on a vector v can be computed without explicitly constructing the matrix by the following observation:

$$\begin{aligned} Av = (P_\Gamma K_\Gamma + P_{\Gamma\Omega} K_{\Omega\Gamma})v &= \begin{pmatrix} P_\Gamma & P_{\Gamma\Omega} \end{pmatrix} \begin{pmatrix} K_\Gamma \\ K_{\Omega\Gamma} \end{pmatrix} v \\ &= \begin{pmatrix} P_\Gamma & P_{\Gamma\Omega} \end{pmatrix} \begin{pmatrix} K_\Gamma & K_{\Gamma\Omega} \\ K_{\Omega\Gamma} & K_\Omega \end{pmatrix} \begin{pmatrix} v \\ 0 \end{pmatrix}. \end{aligned} \tag{4.1}$$

Let $\tilde{v}$ be the vector $\begin{pmatrix} v & 0 \end{pmatrix}^T$ reordered lexicographically and let K represent the last matrix in (4.1) reordered correspondingly. Since K then has a multi level Toeplitz structure, it can be applied using a standard embedding technique. The arithmetic complexity is $\mathcal{O}(n_c^2 N_{\bar{\Omega}} \log N_{\bar{\Omega}})$ and the memory requirement is $\mathcal{O}(n_c^2 N_{\bar{\Omega}})$.

The matrix $\begin{pmatrix} P_\Gamma & P_{\Gamma\Omega} \end{pmatrix}$ is $n_c N_\Gamma \times n_c N_{\bar{\Omega}}$ and sparse, so a matrix vector multiplication is obtained in $\mathcal{O}(n_c^2 N_\Gamma)$ operations. The over all complexity and memory consumption is hence dominated by the application of K. The technique described above is also used when computing the right hand side g in (3.5).

Any iterative method for non symmetric problems can now be applied, provided it does not require explicit access to the matrix. When using an iterative method, it is common to use the norm of the residual in a criterion for when to terminate the iterations. By the following theorem, it is easy to monitor the residual of the original system when iterating on the reduced system, without any additional computations.

THEOREM 4.1. *If u is a vector satisfying*

$$u = \begin{pmatrix} u_\Gamma \\ u_\Omega \end{pmatrix} = \begin{pmatrix} K_\Gamma & K_{\Gamma\Omega} \\ K_{\Omega\Gamma} & K_\Omega \end{pmatrix} \begin{pmatrix} v_\Gamma \\ f_\Omega \end{pmatrix},$$

for some v_Γ, then the residuals satisfy

$$r_{\bar{\Omega}} \equiv Pu - f = \begin{pmatrix} Av_\Gamma - g \\ 0 \end{pmatrix} \equiv \begin{pmatrix} r_\Gamma \\ 0 \end{pmatrix},$$

where A and g are given by (3.6).

PROOF.

$$\begin{aligned} Pu - f &= \begin{pmatrix} P_\Gamma & P_{\Gamma\Omega} \\ P_{\Omega\Gamma} & P_\Omega \end{pmatrix} \begin{pmatrix} u_\Gamma \\ u_\Omega \end{pmatrix} - \begin{pmatrix} f_\Gamma \\ f_\Omega \end{pmatrix} \\ &= \begin{pmatrix} P_\Gamma & P_{\Gamma\Omega} \\ P_{\Omega\Gamma} & P_\Omega \end{pmatrix} \begin{pmatrix} K_\Gamma & K_{\Gamma\Omega} \\ K_{\Omega\Gamma} & K_\Omega \end{pmatrix} \begin{pmatrix} v_\Gamma \\ f_\Omega \end{pmatrix} - \begin{pmatrix} f_\Gamma \\ f_\Omega \end{pmatrix} \\ &= \begin{pmatrix} P_\Gamma K_\Gamma + P_{\Gamma\Omega} K_{\Omega\Gamma} & P_\Gamma K_{\Gamma\Omega} + P_{\Gamma\Omega} K_\Omega \\ 0 & I \end{pmatrix} \begin{pmatrix} v_\Gamma \\ f_\Omega \end{pmatrix} - \begin{pmatrix} f_\Gamma \\ f_\Omega \end{pmatrix} \\ &= \begin{pmatrix} Av_\Gamma - g \\ 0 \end{pmatrix}. \end{aligned}$$

□

Besides the application of A, which is needed inside the iterative method of choice, there is a setup phase and a post processing phase involved in order to obtain the solution of the original problem. The setup phase consists of the computation of the fundamental solution, which is done in $\mathcal{O}(n_c^2 N_{\bar{\Omega}} \log N_{\bar{\Omega}})$ arithmetic operations, and of the reduced right hand side, which is done in the same fashion as the application of A, and with the same complexity. Also the post processing, i.e. computing u from v in (3.4) is of the same complexity as the application of A.

The application technique described above relies on that the domain is a uniform grid arranged in a hypercube. Note though that even if the domain of interest is irregular, it can often be embedded in a hypercube, and boundary conditions can then be implemented by e.g. interpolation techniques. This approach is taken in section 8.

5 PDE problems

Assume that the underlying problem is a well posed linear PDE with constant coefficients, posed on a d-dimensional unit hypercube. Such an equation can be written in abstract notation as

$$\begin{cases} \mathbf{P_\Omega u}(x) = \mathbf{f_\Omega}(x), & x \in \mathbf{\Omega} \subset \mathbb{R}^d \\ \mathbf{P_\Gamma}(x)\mathbf{u}(x) = \mathbf{f_\Gamma}(x), & x \in \mathbf{\Gamma} \subset \partial\mathbf{\Omega}, \end{cases} \tag{5.1}$$

where $\mathbf{P_\Omega}$ and $\mathbf{P_\Gamma}$ are differential operators,[1] $\mathbf{u}$ is an unknown, vector valued function with n_c components, $\mathbf{f_\Omega}$ is the right hand side, $\mathbf{f_\Gamma}$ specifies boundary conditions, $\mathbf{\Omega}$ is the hypercube, and $\mathbf{\Gamma}$ is the set where boundary conditions are imposed. Note that the operator $\mathbf{P_\Gamma}$ is allowed to vary along the boundary.

If (5.1) is discretized using finite differences on a uniform grid, we obtain a linear system of equations that can be represented by (2.3), where $\begin{pmatrix} P_{\Omega\Gamma} & P_\Omega \end{pmatrix}$ corresponds to the discretization of $\mathbf{P_\Omega}$.

Let the mesh have $n_k + 1$ grid-points in dimension k and

$$x_i = (x_{i_1}, \ldots, x_{i_d}) = (i_1 h_1, \ldots i_d h_d),$$

[1] If more than one set of boundary conditions is imposed at the same position, $\mathbf{P_\Gamma}$ in 5.1 needs a rather generous interpretation. However, we do not need a more complicated notation to explain the reduction process.

where $h_k = 1/n_k$. In general, $i \in \Gamma$ does *not* imply $x_i \in \mathbf{\Gamma}$, for two reasons. First, the discretization of $\mathbf{P_\Omega}$ might be such that it needs to be modified at one or several grid-points near the boundary $\partial\mathbf{\Omega}$. Hence, $\hat{P}$ will not be applied in such grid-points, implying that they belong to Γ although they have a non-zero distance to $\mathbf{\Gamma}$. The other reason is that the boundary conditions can be eliminated, so that the difference operator at the outermost grid-points is a mix of discretizations of $\mathbf{P_\Omega}$ and $\mathbf{P_\Gamma}$. In that case, i corresponding to $x_i \in \mathbf{\Gamma}$ is not even a member of Γ.

As an example, we use Poisson's equation on the unit square with both Dirichlet and Neumann boundary conditions.

$$\text{(5.2)} \qquad \begin{cases} \Delta\mathbf{u}(x) = \mathbf{f_\Omega}(x), & x \in \mathbf{\Omega} = (0,1)^2 \\ \mathbf{u}(x) = \mathbf{f_\Gamma}(x), & \begin{cases} x_1 \in (0,1), & x_2 = 0, \\ x_1 \in (0,1), & x_2 = 1, \\ x_1 = 1, & x_2 \in (0,1), \end{cases} \\ -\frac{\partial}{\partial x_1}\mathbf{u}(x) = \mathbf{f_\Gamma}(x), & x_1 = 0, x_2 \in (0,1). \end{cases}$$

A straight forward discretization of (5.2), with $n_1 = n_2 = n = 1/h$, where the boundary conditions are left as separate equations would be

$$\text{(5.3)} \qquad \begin{cases} \hat{P}u_i = \mathbf{f_\Omega}(x_i), & i \in \Omega = (1,\dots,n-1)^2, \\ u_i = \mathbf{f_\Gamma}(x_i), & \begin{cases} i_1 = 1,\dots,n-1, & i_2 = 0, \\ i_1 = 1,\dots,n-1, & i_2 = n, \\ i_1 = n, & i_2 = 1,\dots,n-1, \end{cases} \\ -\frac{u_{(1,i_2)} - u_{(0,i_2)}}{h} = \mathbf{f_\Gamma}(x_{(0,i_2)}), & i_2 = 1,\dots,n-1, \end{cases}$$

where $\hat{P}u_i = (-4u_i + u_{(i_1-1,i_2)} + u_{(i_1+1,i_2)} + u_{(i_1,i_2-1)} + u_{(i_1,i_2+1)})/h^2$. In this case, we have $x_i \in \mathbf{\Gamma} \Leftrightarrow i \in \Gamma$ and $x_i \in \mathbf{\Omega} \Leftrightarrow i \in \Omega$.

The same discretization, but with eliminated boundary conditions is somewhat more complicated to write down. The operator $\hat{P}$ is unchanged, but the definitions of Ω, Γ, f_Ω, and f_Γ are different. We have $\Omega = (2,\dots,n-2)^2$ and as examples we show the equations connected to the south and west boundaries.

$$\text{(5.4)} \qquad \begin{aligned} \frac{-4u_{(i_1,1)} + u_{(i_1-1,1)} + u_{(i_1+1,1)} + u_{(i_1,2)}}{h^2} &= f_{\Gamma,(i_1,1)}, \quad i_1 = 2,\dots,n-2, \\ \frac{-3u_{(1,i_2)} + u_{(2,i_2)} + u_{(1,i_2-1,1)} + u_{(1,i_2+1)}}{h^2} &= f_{\Gamma,(1,i_2)}, \quad i_2 = 2,\dots,n-2, \end{aligned}$$

where

$$\begin{aligned} f_{\Gamma,(i_1,1)} &= \mathbf{f_\Omega}(x_{(i_1,1)}) - \mathbf{f_\Gamma}(x_{(i_1,0)})/h^2, \quad i_1 = 2,\dots,n-2, \\ f_{\Gamma,(1,i_2)} &= \mathbf{f_\Omega}(x_{(1,i_2)}) - \mathbf{f_\Gamma}(x_{(0,i_2)})/h, \quad i_2 = 2,\dots,n-2. \end{aligned}$$

To exemplify the connection between BIE and our reduced system, we use the Poisson example, but for simplicity with $\mathbf{f_\Omega} = 0$ and with only Dirichlet boundary conditions,

$$\text{(5.5)} \qquad \begin{cases} \Delta\mathbf{u}(x) = 0, & x \in \mathbf{\Omega} \\ \mathbf{u}(x) = \mathbf{f_\Gamma}(x), & x \in \mathbf{\Gamma} = \partial\mathbf{\Omega}. \end{cases}$$

By discretizing and not eliminating the boundary conditions, we obtain algebraic equations almost like (5.3), and on matrix form we have

$$\begin{pmatrix} I & 0 \\ P_{\Omega\Gamma} & P_\Omega \end{pmatrix} \begin{pmatrix} u_\Gamma \\ u_\Omega \end{pmatrix} = \begin{pmatrix} f_\Gamma \\ 0 \end{pmatrix}.$$

The reduced matrix is in this case $A = K_\Gamma$, c.f. (3.6), and the reduced right hand side is $g = f_\Gamma$. The reduced system can hence be written

$$\sum_{j\in\Gamma} E_{i-j} v_{\Gamma,j} = f_{\Gamma,i}, \quad i \in \Gamma, \tag{5.6}$$

and the solution of the original equations is

$$u_i = \sum_{j\in\Gamma} E_{i-j} v_{\Gamma,j}, \quad i \in \bar{\Omega}. \tag{5.7}$$

A continuous counterpart is the single layer potential

$$\mathbf{u}(x) = \int_\Gamma \mathbf{E}(x-y)\mathbf{v}(y)dy, \quad x \in \mathbf{\Omega}, \tag{5.8}$$

where $\mathbf{E}$ is a fundamental solution of $\mathbf{\Delta}$ and $\mathbf{v}$ is the solution of the BIE

$$\int_\Gamma \mathbf{E}(x-y)\mathbf{v}(y) = \mathbf{f_\Gamma}(x), \quad x \in \mathbf{\Gamma}. \tag{5.9}$$

It is easy to see that, in this simple case, (5.6) and (5.7) are first order discretizations of (5.9) and (5.8), respectively.

In the following sections, we present numerical experiments on the reduced system that arises when the original problem is a discretization of a linear PDE with constant coefficients. The experiments are chosen to examine how the behavior of GMRES depends on problem size, PDE-parameters, discretization parameters, and boundary conditions for some first and second order scalar PDE and a hyperbolic system of PDE. We also present a convergence analysis for a simpler iterative method applied to one specific case.

Common to all iterative experiments is that we use the zero vector as initial guess and that we iterate until the residual norm is decreased by a factor of 10^6, i.e. until

$$\|r_\Omega^m\| \leq 10^{-6}\|f_{\bar{\Omega}}\|,$$

which by Theorem 4.1 implies that the condition to use for the reduced residual is

$$\|r_\Gamma^m\| \leq 10^{-6}\|f_{\bar{\Omega}}\|, \tag{5.10}$$

if the norm is one that satisfies $\| \begin{pmatrix} v & 0 \end{pmatrix}^T \| = \|v\|$. In all experiments using GMRES, we use the 2-norm.

6 Scalar PDE on a Square

In this section, we consider first and second order PDE-problems posed on the unit square. Hence, $\mathbf{\Omega} = (0,1)^2$ through out the section.

First Order PDE

The convection equation

$$\begin{cases} \left(b_1 \frac{\partial}{\partial x_1} + b_2 \frac{\partial}{\partial x_2}\right) \mathbf{u}(x) = \mathbf{f}_{\mathbf{\Omega}}(x), & x \in \mathbf{\Omega}, \\ \mathbf{u}(x_1, 0) = \mathbf{f}_{\mathbf{\Gamma}}(x_1, 0), & x_1 \in (0,1), \\ \mathbf{u}(0, x_2) = \mathbf{f}_{\mathbf{\Gamma}}(0, x_2), & x_2 \in (0,1), \end{cases}$$

is discretized with standard centered finite differences with artificial viscosity of strength γ, i.e.

$$\hat{P} = b_1 \left(D_0^{x_1} - \frac{\gamma h_1}{2} D_+^{x_1} D_-^{x_1} \right) + b_2 \left(D_0^{x_2} - \frac{\gamma h_2}{2} D_+^{x_2} D_-^{x_2} \right). \tag{6.1}$$

The boundary conditions are eliminated, implying that

$$\begin{aligned} \Omega &= (2, \ldots, n_1 - 2) \times (2, \ldots, n_2 - 2), \\ \bar{\Omega} &= (1, \ldots, n_1 - 1) \times (1, \ldots, n_2 - 1), \\ \Gamma &= \bar{\Omega} \setminus \Omega. \end{aligned} \tag{6.2}$$

In the experiments we use

$$\begin{aligned} \mathbf{f}_{\mathbf{\Omega}}(x) &= \begin{cases} e^{-20r^2}, & x_2 \le 1/2, \\ x_1, & x_2 > 1/2, \end{cases} \\ \mathbf{f}_{\mathbf{\Gamma}}(x) &= \begin{cases} 1, & x_2 = 0, \\ 0, & x_1 = 0, \end{cases} \end{aligned} \tag{6.3}$$

where r is the distance from x to the center of the square.

The first experiment shows the number of GMRES iterations needed to obtain convergence according to (5.10) for the original system and for the corresponding reduced system. In the reduction process, we use $E = E^L$, c.f. Section 3.

The results are shown in Table 6.1, where we use $b_1 = b_2 = 1$.

Table 6.1: Iteration counts for GMRES on the original system (P) and the reduced system (A) for $b_1 = b_2 = 1$.

	$\gamma = 1/16$		$\gamma = 1/8$		$\gamma = 1/4$		$\gamma = 1/2$	
$n_1 = n_2$	P	A	P	A	P	A	P	A
32	160	39	109	29	83	20	70	13
64	226	42	172	30	146	20	133	13
128	351	41	297	29	272	20	259	13
256	601	39	548	29	525	19	514	13
512	-	38	-	27	-	19	-	13
1024	-	37	-	26	-	19	-	13

It is obvious from Table 6.1 that the reduced system shows much better convergence properties than the original system, both in terms of absolute iteration counts and in the grid independent behavior. Without the reduction, it was not even possible to solve the problem without restarting on the largest grids.

Table 6.2 shows results for different directions of the convective field. We use $(b_1, b_2) = \sqrt{2}(\cos\Theta, \sin\Theta)$, and $\gamma = 1/2$.

Table 6.2: Iteration counts for GMRES on the reduced system for various directions of the convective field.

$n_1 = n_2$	$\Theta = \pi/16$	$\Theta = \pi/4$	$\Theta = 7\pi/16$
32	14	13	14
64	14	13	16
128	14	13	18
256	14	13	20
512	14	13	22
1024	13	13	24

The reason for the differences in the $\Theta = \pi/16$ and $\Theta = 7\pi/16$ columns is that the construction of E^L is not symmetric with respect to the coordinate axes. Periodic boundary conditions are used in the x_2-, but not in the x_1-direction. The results in Table 6.2 indicate grid independent convergence, except if the convective field is almost aligned with the coordinate axis along which the fundamental solution is periodic.

Using $n_1 \neq n_2$ in various ways yields the results in Table 6.3, where $b_1 = b_2 = 1$ and $\gamma = 1/2$. We conclude that the iterative behavior does not rely on square grid-cells or on a fixed aspect ratio.

Table 6.3: Iteration counts for GMRES on the reduced system for $b_1 = b_2 = 1$ and $\gamma = 1/2$.

n	$n_1 = n$ $n_2 = 2n$	$n_1 = 64$ $n_2 = n$	$n_1 = n$ $n_2 = 64$
32	13	13	13
64	14	13	13
128	14	14	14
256	13	14	14
512	13	14	14
1024	13	14	14

Second Order PDE

As a representative for second order scalar PDE-problems, we take the convection diffusion equation

$$\text{(6.4)} \qquad \begin{cases} \left(-\varepsilon_1 \frac{\partial^2}{\partial x_1^2} - \varepsilon_2 \frac{\partial^2}{\partial x_2^2} + b_1 \frac{\partial}{\partial x_1} + b_2 \frac{\partial}{\partial x_2}\right) \mathbf{u}(x) = \mathbf{f}_{\mathbf{\Omega}}(x), & x \in \mathbf{\Omega}, \\ \mathbf{u}(x) = \mathbf{f}_{\mathbf{\Gamma}}(x), & x \in \mathbf{\Gamma}_1, \\ \frac{\partial}{\partial \nu}\mathbf{u}(x) = \mathbf{f}_{\mathbf{\Gamma}}(x), & x \in \mathbf{\Gamma}_2, \end{cases}$$

where $\Gamma_1 \cup \Gamma_2 = \partial\Omega$, $\Gamma_1 \cap \Gamma_2 = \emptyset$ and ν is the outward pointing normal vector. Equation (6.4) is discretized using second order centered finite differences,

$$\hat{P} = -\varepsilon_1 D_+^{x_1} D_-^{x_1} - \varepsilon_2 D_+^{x_2} D_-^{x_2} + b_1 D_0^{x_1} + b_2 D_0^{x_2}.$$

The boundary conditions are eliminated, end the equations for $i \in \Gamma$ are obtained along the lines shown in (5.4).

Experiments are performed both for the pure Dirichlet case, in which $\mathbf{\Gamma}_2 = \emptyset$, and for a Dirichlet-Neumann case, where $\mathbf{\Gamma}_2 = \{(x_1, 1)|x_1 \in (0,1)\} \cup \{(1, x_2)|x_2 \in (0,1)\}$, i.e. the north and east part of $\mathbf{\Gamma}$. In both cases we use

$$\mathbf{f}_{\mathbf{\Gamma}} = \begin{cases} 0, & x \in \text{ east and west boundary}, \\ 1, & x \in \text{ south and north boundary}, \end{cases}$$

and the same $\mathbf{f}_{\mathbf{\Omega}}$ as in (6.3).

Tables 6.4 and 6.5 show iteration counts using $E = E^L$, examining how GMRES behaves depending on the viscosity parameters ε_1 and ε_2 when $b_1 = b_2 = 1$.

Table 6.4: Iteration counts for GMRES on the reduced system for $\varepsilon_1 = \varepsilon_2 = \varepsilon$.

	Dirichlet			Dirichlet-Neumann		
$n_1 = n_2$	$\varepsilon = 0.001$	$\varepsilon = 0.1$	$\varepsilon = 10$	$\varepsilon = 0.001$	$\varepsilon = 0.1$	$\varepsilon = 10$
32	31*	13	14	30*	14	18
64	25*	17	17	23*	18	23
128	18*	23	22	16*	24	29
256	13*	29	28	11*	31	36
512	8	37	35	8	39	45
1024	10	46	44	9	50	56

Table 6.5: Iteration counts for GMRES on the reduced system for $\varepsilon_1 \neq \varepsilon_2$.

	Dirichlet		Dirichlet-Neumann	
$n_1 = n_2$	$\varepsilon_1 = 1$ $\varepsilon_2 = 0.01$	$\varepsilon_1 = 0.01$ $\varepsilon_2 = 1$	$\varepsilon_1 = 1$ $\varepsilon_2 = 0.01$	$\varepsilon_1 = 0.01$ $\varepsilon_2 = 1$
32	26*	22*	30*	25*
64	32	28	39	31
128	45	36	51	39
256	57	45	66	51
512	73	56	83	65
1024	92	70	104	80

In cases marked with a *, the computations are irrelevant from a PDE point of view, since the solution contains unphysical oscillations near the boundary, due to that the condition on the mesh Péclet number is violated, see [7].

The results in Table 6.4 indicate that for isotropic second order equations, the GMRES applied to the reduced system does show a grid dependent behavior, but that the increase in numbers of iterations is rather mild. The fastest convergence seems to occur close to the point where the mesh Péclet number condition met. It is interesting to note that when the boundary layers are resolved, a smaller viscosity parameter often gives lower iteration counts, as opposed to most other methods that benefit from large viscosity. Note also that Dirichlet and Dirichlet-Neumann boundary conditions work equally well in the isotropic case.

The results are somewhat degraded in the anisotropic case, which is shown in Table 6.5.

7 Convergence Analysis

The most encouraging result from the experiments in the first part of section 6 was the grid independent convergence for GMRES when applied to the reduced system corresponding to the discretization (6.1). For the special case $b_1 = b_2 = \gamma = 1$, we can also analyze the 1-norm of $I - A$ in detail. We prove a theorem implying that even a fixed-point iterative method converges in a low number of iterations, independent of the problem size. To prove the theorem we need the following lemmas.

LEMMA 7.1. *If P and K are multi-level Toeplitz matrices, then*

$$\|I - KP\|_\infty = \|I - PK\|_1.$$

PROOF. Multi-level Toeplitz matrices, as well as ordinary Toeplitz matrices, belong to the class of persymmetric matrices, see [5], i.e. if K has such structure, it satisfies

$$K^T = XKX,$$

where X is the exchange matrix,

$$X = \begin{pmatrix} 0 & \cdots & 0 & 1 \\ \vdots & & 1 & 0 \\ & & & \vdots \\ 0 & 1 & & \\ 1 & 0 & \cdots & 0 \end{pmatrix}.$$

It is easy to see that $X = X^{-1}$. Hence

$$\begin{aligned} \|I - KP\|_\infty &= \|(I - KP)^T\|_1 = \|I - P^T K^T\|_1 = \|X(I - P^T K^T)X)\|_1 \\ &= \|I - XP^T XXK^T X\|_1 = \|I - PK\|_1, \end{aligned}$$

where we have also used that multiplying a matrix by X from left or right does not change the 1-norm, since X is a permutation matrix. □

LEMMA 7.2. *In a lexicographical ordering, the matrix P representing (6.1) together with eliminated Dirichlet boundary conditions and with $b_1 = b_2 = \gamma = 1$, has multi-level Toeplitz structure.*

PROOF. The discretization can in the current setting be written as

$$\begin{cases} (D_-^{x_1} + D_-^{x_2})v_i = f_{\Omega,i}, & i \in \Omega, \\ (D_-^{x_1} + h_2^{-1})v_{(1,i_2)} = f_{\Gamma,(1,i_2)}, & i_2 = 2, \ldots, n_2 - 1, \\ (h_1^{-1} + D_-^{x_2})v_{(i_1,1)} = f_{\Gamma,(i_1,1)}, & i_1 = 2, \ldots, n_1 - 1, \\ (h_1^{-1} + h_2^{-1})v_{(1,1)} = f_{\Gamma,(1,1)}. \end{cases}$$

The left hand side is in the lexicographical ordering represented by the coefficient matrix

$$\begin{pmatrix} P_1 & \cdots & \cdots & 0 \\ -h_2^{-1}I & P_1 & & \vdots \\ \vdots & \ddots & \ddots & \vdots \\ 0 & \cdots & -h_2^{-1}I & P_1 \end{pmatrix},$$

where

$$P_1 = \begin{pmatrix} h_1^{-1} + h_2^{-1} & \cdots & \cdots & 0 \\ -h_2^{-1} & h_1^{-1} + h_2^{-1} & & \vdots \\ \vdots & \ddots & \ddots & \vdots \\ 0 & \cdots & -h_2^{-1} & h_1^{-1} + h_2^{-1} \end{pmatrix}.$$

□

THEOREM 7.3. *Let P be the matrix representing (6.1) in a lexicographical ordering together with eliminated Dirichlet boundary conditions and with $b_1 = b_2 = \gamma = 1$ and $n_1 = n_2 = n$. Let K be the matrix representing (3.2) in the same ordering, with $E = E^D$, and let A be the reduced matrix that corresponds to P and K. Then*

$$\|I - A\|_1 \leq c(n) \leq 2/3.$$

PROOF. Clearly it holds that

$$\|I - A\|_1 \leq \left\| \begin{pmatrix} I - A & P_\Gamma K_{\Gamma\Omega} + P_\Gamma \Omega K_\Omega \\ 0 & 0 \end{pmatrix} \right\|_1 = \|I - PK\|_1,$$

and hence, by Lemma 7.1 and 7.2, that

$$\|I - A\|_1 \leq \|I - KP\|_\infty,$$

since K has multi level Toeplitz structure by construction. In [1], it is shown that for the present setting,

$$\|I - KP\|_\infty < \frac{1}{2} \frac{1}{1 - (1 + 1/n)^{-2n}} = c(n),$$

which is a decreasing function less then 2/3 for all positive n. □

Table 7.1 shows the norms of $I - A$ in the setting of Theorem 7.3, both when the reduction is obtained using E^D, as in the theorem, and when E^L is used. The bound given in the proof is also shown.

Table 7.1:

n	$c(n)$	$\|I - A\|_1$, E^D	$\|I - A\|_1$, E^L
16	0.584	0.298	0.516
32	0.581	0.354	0.552
64	0.580	0.396	0.563
128	0.579	0.426	0.570
256	0.579	0.447	0.574

8 Non-Square Regions

The reduction technique works also for non-square regions. The easiest generalization, from an implementational point of view, is when the domain has straight boundaries that coincide with grid-lines. As an example we use the unit square with the upper right quarter removed, i.e. an L-shaped domain. We use the convection diffusion equation described in section 6, together with Dirichlet boundary conditions.

The L-shaped region is embedded in the unit square, whose interior is discretized with odd numbers of grid-points in each dimension, i.e. n_1 and n_2 are chosen to be even. Figure 8.1 shows an example, where $n_1 = n_2 = 16$. As before, the boundary conditions are eliminated, implying that Γ consists of the grid-points denoted by filled bullets in Figure 8.1. Empty bullets denote grid-points belonging to Ω and crosses denote the grid-points that are present only due to the embedding procedure.

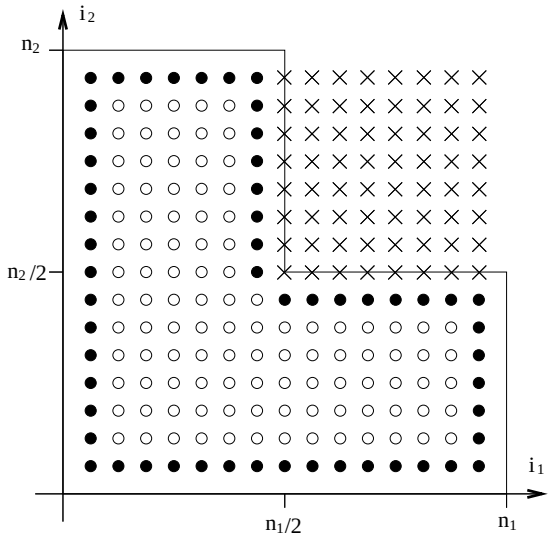

Figure 8.1: The L-shaped domain. Empty bullets denote grid-points in Ω, filled bullets denote grid-points in Γ, and crosses denote irrelevant grid-points.

In the numerical experiments, we use the restriction of $\mathbf{f_\Omega}$ in (6.3) to the L-shaped domain, and

$$\mathbf{f_\Gamma} = \begin{cases} 0, & x \in \text{ boundaries facing east and west,} \\ 1, & x \in \text{ boundaries facing south and north.} \end{cases}$$

A solution is plotted in Figure 8.2, where the grid-points denoted by crosses in Figure 8.1 have been removed. The values of the solution at the boundaries have been added to the plot separately.

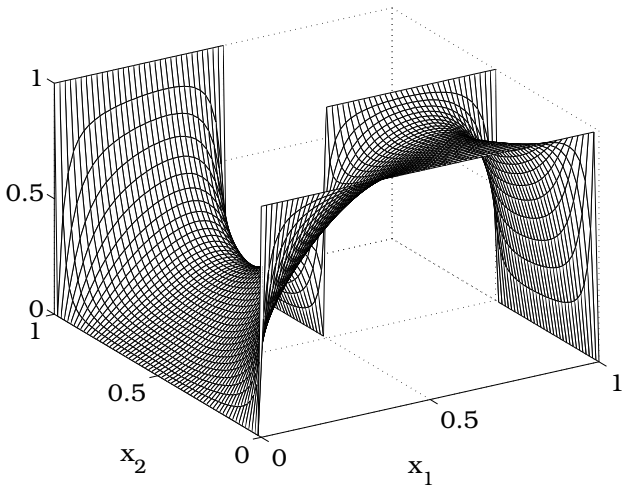

Figure 8.2: Solution of convection diffusion equation, $\varepsilon = 0.1$ on an L-shaped domain.

Table 8.1: Iteration counts for GMRES on the reduced system corresponding to the convection diffusion equation on an L-shaped domain.

$n_1 = n_2$	$\varepsilon = 0.001$	$\varepsilon = 0.1$	$\varepsilon = 10$
32	35*	14	14
64	26*	18	19
128	18*	23	24
256	13*	30	30
512	8	38	38
1024	10	47	47

Table 8.1 shows iteration counts for GMRES on the reduced problem for the L-shaped domain. By comparing to Table 6.4, we see that the iterative behavior is very similar to the square case. Again, the asterisks indicate that the condition on the mesh Péclet number is violated.

It is also possible to deal with PDE-problems posed on regions where the boundary is not aligned with the grid. As an example we use the same convection-diffusion equation as above, but posed on a circle inscribed in the unit square. Dirichlet boundary conditions are used. The discretization of the differential operator is performed as before in the interior, but the boundary conditions need a different treatment. The simplest approach would be to prescribe values of the solution at the grid-point closest to the circle, but that would lead to an undesirable staircase effect on coarse grids. Instead, we use an embedded boundary technique where boundary conditions are implemented using interpolation

whenever any part of the stencil refers to a grid-point outside the boundary. Figure 8.3 shows an example, where the Dirichlet boundary condition is implemented as

$$\begin{aligned}(1-\alpha)u_{(i_1,i_2)} + \alpha u_{(i_1+1,i_2)} &= \mathbf{f}_{\mathbf{\Gamma}}(x_i + (\alpha h_1, 0)), \quad \alpha > h_1,\\ u_i &= \mathbf{f}_{\mathbf{\Gamma}}(x_i + (\alpha h_1, 0)), \quad \alpha \le h_1.\end{aligned}$$

The special treatment of small α is to avoid ill-conditioning of the interpolation. A similar embedded boundary technique is described in [10], but with a different treatment of the case $\alpha \approx 0$.

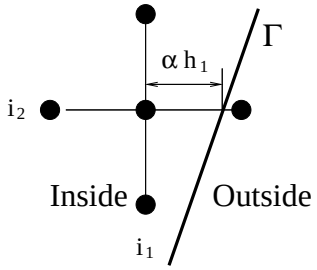

Figure 8.3: The stencil referring to a grid-point outside a non-square region.

The discretized boundary conditions are eliminated, yielding a definition of the sets Ω and Γ which is exemplified in Figure 8.4.

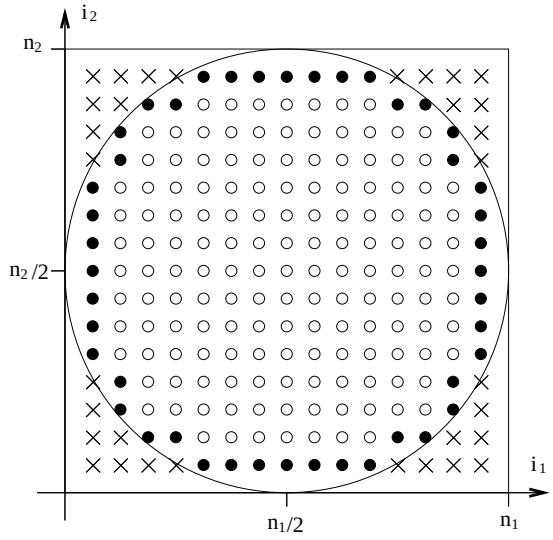

Figure 8.4: The circular domain. Empty bullets denote grid-points in Ω, filled bullets denote grid-points in Γ, and crosses denote irrelevant grid-points.

Table 8.2: Iteration counts for GMRES on the reduced system corresponding to the convection diffusion equation on a circular domain.

$n_1 = n_2$	$\varepsilon = 0.001$	$\varepsilon = 0.1$	$\varepsilon = 10$
32	70*	16	15
64	99*	26	23
128	132*	32	31
256	157*	40	38
512	52	57	53
1024	57	66	62

Table 8.2 shows iteration counts for GMRES on the reduced system when the original problem is the convection-diffusion equation on a circular domain, with boundary conditions implemented as above. We see that the numbers are quite moderate and independent of the viscosity parameter, when the mech Péclet number condition is satisfied. Figure 8.5 shows an example of the solution.

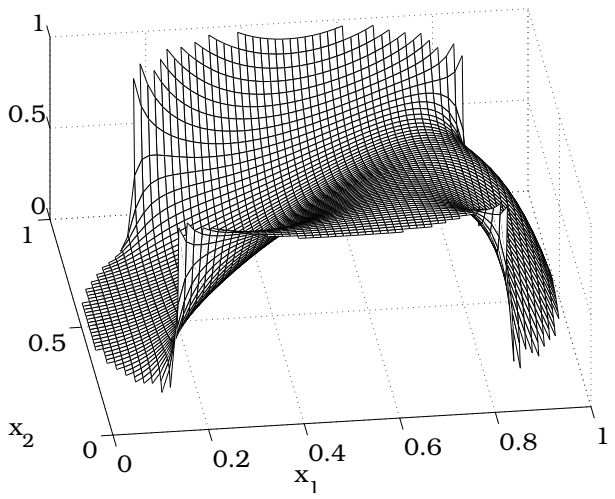

Figure 8.5: Solution of convection diffusion equation on an circular domain, $\varepsilon = 0.1$.

9 Higher Dimensional PDE

The convection equation in Section 6 generalized to d dimensions is

$$\begin{cases} \sum_{k=1}^{d} b_k \frac{\partial}{\partial x_k} \mathbf{u}(x) = \mathbf{f}_{\mathbf{\Omega}}(x), & x \in \mathbf{\Omega} = (0,1)^d, \\ \mathbf{u}(x) = \mathbf{f}_{\mathbf{\Gamma}}(x), & x \in \mathbf{\Gamma}. \end{cases}$$

In this section, we use $b_k = 1$, $k = 1, \ldots, d$,

$$\mathbf{\Gamma} = \bigcup_{k=1}^{d} \{x | x \in \bar{\mathbf{\Omega}}, x_k = 0\},$$

and

$$\begin{aligned} \mathbf{f}_{\mathbf{\Omega}}(x) &= e^{-20r^2}, \quad x \in \mathbf{\Omega}, \\ \mathbf{f}_{\mathbf{\Gamma}}(x) &= 0, \qquad\quad x \in \mathbf{\Gamma}. \end{aligned}$$

The discretization is a straight forward generalization of the two-dimensional case, i.e.

$$\hat{P} = \sum_{k=1}^{d} b_k (D_0^{x_k} - \frac{\gamma h_k}{2} D_+^{x_k} D_-^{x_k}),$$

and the boundary conditions are eliminated as above.

Table 9.1 shows iteration results for GMRES applied to the reduced system with $E = E^L$ and $\gamma = 1/2$, for dimensions from 2 to 6. By comparing the columns, we note that the number of iterations seem to be independent of the number of dimensions. The difference between the first column and Table 6.1 depends on that different boundary conditions and right hand sides are used.

Table 9.1: Iteration counts for GMRES on the reduced system for $d = 2, \ldots, 6$, $n_k = n$, $k = 1, \ldots, d$.

n	$d = 2$	$d = 3$	$d = 4$	$d = 5$	$d = 6$
4	7	8	8	8	8
5	7	8	9	9	9
6	8	9	9	9	9
7	9	9	9	9	9
8	9	9	9	9	
12	10	11	10	10	
24	11	12	12		
48	12	12			
96	12	13			

10 System of PDE

In this section we apply the reduction process to a system of PDE on the unit square. The system is the linearized steady-state isentropic Euler equations, governing inviscid fluid flow. By linearizing around a solution with constant components, we obtain

$$\begin{cases} \left(A_1 \frac{\partial}{\partial x_1} + A_2 \frac{\partial}{\partial x_2}\right) \mathbf{u}(x) = 0, & x \in \mathbf{\Omega} = (0,1)^2, \\ \text{boundary conditions}, & x \in \mathbf{\Gamma}, \end{cases} \tag{10.1}$$

where $\mathbf{u} = (\rho, \mathbf{u_1}, \mathbf{u_2})^T$ contains the departure from the linearization solution $\mathbf{U} = (\mathbf{R}, \mathbf{U_1}, \mathbf{U_2})^T$ in the density and the two velocity components, and

$$A_1 = \begin{pmatrix} \mathbf{U_1} & \mathbf{R} & 0 \\ c^2/\mathbf{R} & \mathbf{U_1} & 0 \\ 0 & 0 & \mathbf{U_1} \end{pmatrix}, \quad A_2 = \begin{pmatrix} \mathbf{U_2} & 0 & \mathbf{R} \\ 0 & \mathbf{U_2} & 0 \\ c^2/\mathbf{R} & 0 & \mathbf{U_2} \end{pmatrix},$$

where the speed of sound satisfies $c = \sqrt{\gamma\beta R^{\gamma-1}}$, $\beta = 2$, $\gamma = 1.4$.

In the experiments we use $\mathbf{U} = (1, 1, 0)^T$ and the boundary conditions

$$\left.\begin{aligned} \rho(0, x_2) + \mathbf{u_1}(0, x_2) &= g_1(x_2) \\ \mathbf{u_2}(0, x_2) &= g_2(x_2) \\ -\rho(1, x_2) + \mathbf{u_1}(1, x_2) &= g_3(x_2) \end{aligned}\right\}, \quad x_2 \in (0, 1), \tag{10.2}$$
$$\mathbf{u_2}(x_1, 0) = \mathbf{u_2}(x_1, 0) = 0, \quad x_1 \in (0, 1),$$

which from a physical point of view implies that the solution to (10.1), (10.2) approximates the departure from subsonic free flow in a square with solid upper and lower walls. The right hand sides used are

$$\begin{aligned} g_1(x_2) &= e^{-10(x_2-1/2)^2}, \\ g_2(x_2) &= \sin(2\pi x_2), \\ g_3(x_2) &= 0. \end{aligned}$$

The discretization scheme is a standard first-order accurate upwind scheme, corresponding to that a matrix model for second-order artificial viscosity is used. This ensures that upwind differencing is employed for the characteristic solution variables. Let

$$\Lambda_\nu = T_\nu^{-1} A_\nu T_\nu, \quad \nu = 1, 2,$$

be a diagonalization of A_ν and define

$$|A_\nu| \equiv T_\nu |\Lambda_\nu| T_\nu^{-1}.$$

Here, $|\Lambda_\nu| = \mathrm{diag}(|\lambda_{\nu,1}| \ldots |\lambda_{\nu,n_c}|)$, where $\lambda_{\nu,i}$, $1 \le i \le n_c$, denote the eigenvalues of A_ν. For the interior grid points, the upwind difference operator is given by

$$A_\nu D_0^{x_\nu} - \frac{1}{2}|A_\nu| h_\nu D_+^{x_\nu} D_-^{x_\nu}, \quad \nu = 1, 2, \tag{10.3}$$

where $h_\nu = 1/n_\nu$ is the space step. The stencil, cf. (2.2), is defined by

$$\begin{aligned} B_{0,0} &= \tfrac{1}{h_1}|A_1| + \tfrac{1}{h_2}|A_2|, \\ B_{\pm 1,0} &= \tfrac{1}{2h_1}\left(\mp A_1 - |A_1|\right), \ . \\ B_{0,\pm 1} &= \tfrac{1}{2h_2}\left(\mp A_2 - |A_2|\right). \end{aligned}$$

In order to close the system, the boundary conditions (10.2) are complemented by a constant extrapolation of characteristic variables. As before, the boundary conditions are eliminated, giving an original system with $n_c(n_1 - 1)(n_2 - 1)$ unknowns, where $n_c = 3$. The reduced system has $2n_c(n1 + n2 - 2)$ unknowns,

and the reduction is obtained using the fundamental solution $E = E^L$. Iteration results for the reduced system are shown in Table 10.1. Figure 10.1 shows the velocity components of the solution, i.e. the departure from the linearization solution. In the same way, Figure 10.2 shows the density component.

Table 10.1: Iteration counts for GMRES on the reduced system corresponding to an upwind discretization of the Euler equations.

n	$n_1 = n_2 = n$	$n_1 = 64$, $n_2 = n$	$n_1 = n$, $n_2 = 64$
16	15	17	19
32	18	20	21
64	22	22	22
128	24	24	23
256	26	25	25
512	27	26	26
1024	27	27	26

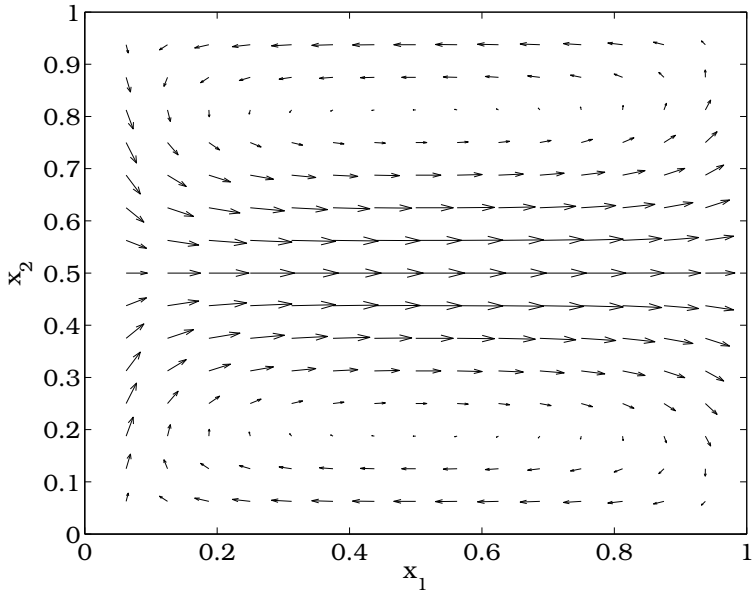

Figure 10.1: The departure from free stream in the velocity field.

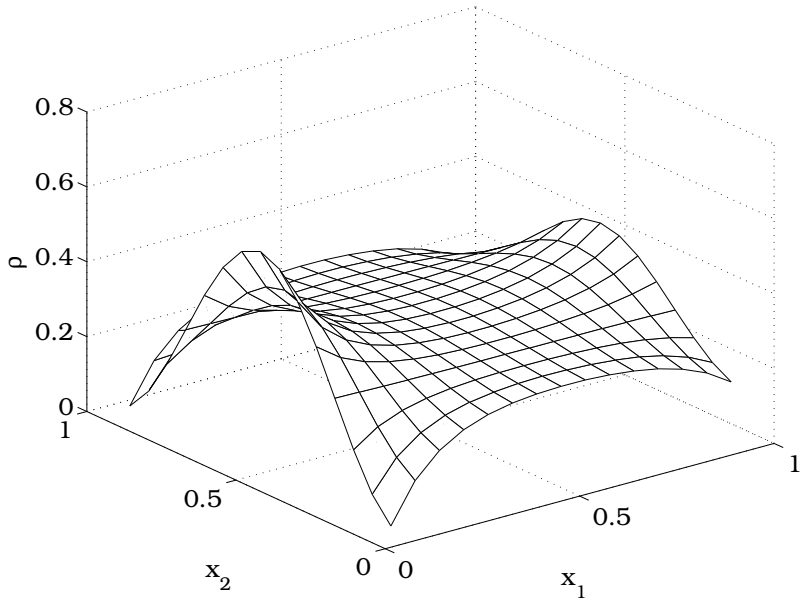

Figure 10.2: The departure from the linearization solution in the density component.

In Table 10.1 we see that that the number of iterations levels out as the problem size increases, and that the iterative behavior does not depend on the aspect ratio of the grid. We conclude that the reduced system is well suited for itarative solution, also for this more applied problem.

11 Summary

A reduction process for difference equations is proposed, where the number of unknowns is reduced to a number corresponding to the boundary of the domain on which the difference equation is posed. The reduced system is related to a boundary integral equation, and it is well suited for iterative methods. Discrete fundamental solutions are used to obtain the reduction.

The coefficient matrix in the reduced system can be applied efficiently by the use of FFT. Since no more complex operations are needed, each iteration is performed in $\mathcal{O}(N \log N)$ arithmetic operations, where N is the number of unknowns in the original formulation of the difference equation.

A convergence proof is given for a special case and numerous numerical experiments are performed on discretizations of various PDE problems, includig scalar equations and systems, square and non-square regions, and higher dimensional problems. The results indicate that first order PDEs, scalar as well as systems, yield grid independent convergence.

GMRES is successfully applied to the reduced equations corresponding to the linearized steady state Euler equations, discretized with an upwind scheme.

REFERENCES

1. H. Brandén, S. Holmgren, and P. Sundqvist, *Discrete Fundamental Solution Preconditioning for Hyperbolic Systems of PDE*, Tech. Rep. 2003-006, Dept. of Information Technology, Uppsala Univ., Uppsala, Sweden, 2003.
2. H. Brandén and P. Sundqvist, *An Algorithm for Computing Fundamental Solutions of Difference Operators.* Accepted for publication in Num. Algorithms, 2004.
3. C. de Boor, K. Höllig, and S. Riemenschneider, *Fundamental solutions for multivariate difference equations*, Amer. J. Math., 111 (1989), pp. 403–415.
4. G. Fairweather and A. Karageorghis, *The Method of Fundamental Solutions for Elliptic Boundary Value problems*, Adv. Comput. Math., 9 (1998), pp. 69–95.
5. G. H. Golub and C. F. V. Loan, *Matrix computations*, The Johns Hopkins University Press, 3 ed., 1996.
6. L. Greengard and V. Rokhlin, *A fast Algorithm for Particle Simulations*, J. Comput. Phys., 73 (1987), pp. 325–348.
7. P. M. Gresho and R. L. Lee, *Don't suppress the wiggles–they're telling you something*, Comput. & Fluids, 9 (1981), pp. 223–253.
8. W. Hackbusch and Z. P. Novak, *On the fast Matrix Multiplication in the Boundary Element Method by Panel Clustering*, Numer. Math., 54 (1989), pp. 463–491.
9. L. Hörmander, *On the Division of Distributions by Polynomials*, Arkiv for Matematik, 54 (1958), pp. 555–568.
10. H.-O. Kreiss, N. A. Petersson, and J. Ystrröm, *Difference Approximations for the Second order Wave equation*, SIAM J. Numer. Anal., 40 (2002), pp. 1940–1967.
11. U. Langer, D. Pusch, and S. Reitzinger, *Efficient Preconditioners for Boundary Element Matrices based on Grey-box Algebraic Muligrid Method.*, Int. J. Numer. Meth. Engng, 58 (2003), pp. 1937–1953.
12. P. G. Martinsson and G. J. Rodin, *Boundary Algebraic Equations for Lattice Problems*, in IUTAM proceedings, Liverpool, UK, 2002.
13. V. S. Ryaben'kii, *Method of Difference Potentials and Its Applications*, Springer Verlag, 2002.
14. E. Tyrtyshnikov, *Mosaic-skeleton Approximations*, Calcolo, 33 (1996), pp. 47–57.